Simulating fields of arbitrary spatial and temporal coherence

Greg Gbur

Department of Physics and Optical Science
University of North Carolina at Charlotte, Charlotte, NC 28223

email: gjgbur@uncc.edu

Abstract: Optical coherence theory typically deals with the average properties of randomly fluctuating fields. However, in some circumstances the averaging process can mask important physical aspects of the field propagation. We derive a new method of simulating partially coherent fields of nearly arbitrary spatial and temporal coherence. These simulations produce the expected coherence properties when averaged over sufficently long time intervals. Examples of numerous fields are given, and an analytic formula for the intensity fluctuations of the field is given. The method is applied to the propagation of partially coherent fields through random phase screens.

OCIS codes: (030.1640) Coherence; (010.1300) Atmospheric propagation

References and links

1. É Verdet, *Leçons d'Optique Physique*, vol. 1, (L'Imprimierie Impériale, Paris, 1869).
2. M. Born and E. Wolf, *Principles of Optics* (Cambridge University Press, Cambridge, 1999, 7th (expanded) edition).
3. L. Mandel and E. Wolf, *Optical Coherence and Quantum Optics* (Cambridge University Press, Cambridge, 1995).
4. J. Wu, "Propagation of a Gaussian-Schell beam through turbulent media," J. Mod. Opt. **37**, 671-684 (1990).
5. G. Gbur and E. Wolf, "Spreading of partially coherent beams in random media," J. Opt. Soc. Am. A **19**, 1592-1598 (2002).
6. J. Wu and A. D. Boardman, "Coherence length of a Gaussian Schell-model beam and atmospheric turbulence," J. Mod. Opt. **38**, 1355-1363 (1991).
7. J. C. Ricklin and F. M. Davidson, "Atmospheric turbulence effects on a partially coherent Gaussian Beam: implications for free-space laser communication," J. Opt. Soc. Am. A **19**, 1794-1802 (2002).
8. O. Korotkova, L. C. Andrews, R. L. Phillips, "A Model for a Partially Coherent Gaussian Beam in Atmospheric Turbulence with Application in Lasercom," Opt. Eng. **43**, 330-341 (2004).
9. L.C. Andrews and R.L. Phillips, *Laser Beam Propagation through Random Media* (SPIE Press, Bellingham, Washington, 1998).
10. M.S. Soskin and M.V. Vasnetsov, *Singular Optics*, in *Progress in Optics*, ed. E. Wolf (Elsevier, Amsterdam), vol. 42 (2001), p. 219-276.
11. G. Gbur, T.D. Visser and E. Wolf, "'Hidden' singularities in partially coherent wavefields", J. Opt. A **6**, S239-S242 (2004).
12. G. Gbur and T.D. Visser, "Phase singularities and coherence vortices in linear optical systems," Opt. Commun. **259**, 428-435 (2006).
13. W. Wang and E. Wolf, "Invariance properties of random pulses and of other random fields in dispersive media," Phys. Rev. E **52**, 5532-5539 (1995).
14. S.O. Rice, *Mathematical analysis of random noise*, in *Selected Papers on Noise and Stochastic Processes*, ed. N. Wax (Dover, NY, 1954).
15. L.C. Andrew and R.L. Phillips, *Laser Beam Scintillation with Applications* (SPIE Press, Bellingham, Washington, 2001).
16. R. Loudon, *The Quantum Theory of Light* (Oxford University Press, Oxford, 1983, 2nd edition).

#72209 - $15.00 USD Received 20 June 2006; revised 21 July 2006; accepted 25 July 2006

17. F.T. Arecchi, E. Gatti and A. Sona, "Time distribution of photons from coherent and Gaussian sources," Phys. Lett. **20**, 27-29 (1966).
18. D.L. Knepp, "Multiple phase-screen calculation of the temporal behavior of stochastic waves," Proc. IEEE **71**, 722-737 (1983).

1. Introduction

Optical coherence theory, which has its origins in studies of the coherence of sunlight [1], is now a well-established discipline in optical science and numerous books [2, 3] deal with the general theory and applications. Optical coherence theory typically deals with the average properties of randomly fluctuating fields. However, the averaging process can in some significant instances mask important physical aspects of the field behavior. For instance, there has been much evidence that partially coherent fields are less susceptible to turbulence degradation than their fully coherent counterparts (see, for instance, [4, 5, 6, 7, 8], and earlier references therein). This has lead to the possibility of using partially coherent fields as sources in free-space optical communications. Such problems, however, involve (at least) three significant time scales: the coherence time of the field, the rate at which turbulence changes with time (the Greenwood frequency), and the data communication rate. Coherence theory calculations involve a long time average over all three scales, masking any possible issues that might arise over finite intervals of time. An example of one such issue is beam wander in turbulence [9].

Other important field properties can be 'hidden' by the averaging process. For instance, in recent years there has been much interest in beams possessing orbital angular momentum, or optical vortices [10]. Such vortices are characterized by an intensity null at their center and a helical phase front, and they are stable under amplitude and phase perturbations of the field. When the vortex field is partially coherent, or its coherence is reduced on propagation through turbulence, the vortex position fluctuates and no point in space, on average, possesses an intensity null. It can be said that the vortex is hidden; it has been shown that some of its behavior is preserved in the correlation properties of the field [11, 12]. At any instant of time, however, the vortex is present in the field.

In this paper we derive a method of numerically generating realizations of partially coherent fields of nearly arbitrary spatial and temporal coherence. The spectral properties, spatial coherence properties, and intensity profile of the field can be freely and independently chosen. The method is an extension and reimagining of a technique [13] used to study the invariance properties of random fields in dispersive media; it may also be considered an extension of techniques for studying random electrical noise [14].

The paper is organized as follows. In section 2 the partially coherent field generator is introduced. In section 3 the intensity fluctuations of the generated field are determined. In section 4 a number of examples of partially coherent fields are described, and their propagation through random phase screens is considered. Section 5 presents concluding remarks.

2. Generating realizations of fields of arbitrary spatial and temporal coherence

The partially coherent field generator is introduced as a generalization of the technique used in Ref. [13] to study the propagation of partially coherent fields in dispersive media; in that reference, only temporal coherence properties were considered. As the goal of this paper is to generate a realization of a field with specified spatial and temporal coherence properties, we first introduce a model of a partially coherent field which can be implemented numerically; we then determine how the parameters of this model are related to the average properties of the partially coherent field.

We consider a source of partially coherent radiation in the plane $z = 0$, which emits optical pulses of fixed spatial and temporal shape at random times. We initially restrict ourselves to a

#72209 - $15.00 USD Received 20 June 2006; revised 21 July 2006; accepted 25 July 2006

time interval $t \in [-T/2, T/2]$. Assuming that the pulses are emitted independently of one another, the probability $p(N)$ that N are emitted in this interval is dictated by Poissonian statistics, i.e.

$$p(N) = \frac{\overline{N}^N}{N!} \exp[-\overline{N}]. \tag{1}$$

Let us assume that N pulses are emitted in this interval. The field of these N pulses is then given by

$$V_N(\mathbf{r},t) = \sum_{j=1}^{N} \Lambda(\mathbf{r}, t - t_j) \exp[-\mathrm{i}\mathbf{K}_j \cdot \mathbf{r}], \tag{2}$$

where $\Lambda(\mathbf{r},t)$ is the field amplitude of a single pulse in the plane $z = 0$ at transverse position $\mathbf{r} = (x,y)$, aside from a linear phase term, t_j is the time of emission of the jth pulse and $\mathbf{K}_j$ is the angle of inclination of the jth pulse. The time of arrival is assumed to be a random variable uniformly distributed throughout the interval, and the angle of inclination is a random variable whose probability distribution $P(\mathbf{K})$ is for now unspecified. This representation of the field is very similar to that used in Ref. [13]; however, the introduction of the angle of inclination $\mathbf{K}_j$ and its probability distribution allows us to control the spatial coherence properties of the field as well as the temporal properties.

Once the pulse shape $\Lambda(\mathbf{r},t)$, the average number of pulses $\overline{N}$ and the probability distribution $P(\mathbf{K})$ are specified, realizations of the field can be generated. We now consider how these quantities are related to the average properties of the field, such as the mutual coherence function.

The mutual coherence function of a statistically stationary field $V(\mathbf{r},t)$ is defined as

$$\Gamma(\mathbf{r}_1, \mathbf{r}_2, \tau) \equiv \langle V^*(\mathbf{r}_1, t_1) V(\mathbf{r}_2, t_2) \rangle, \tag{3}$$

where $\tau \equiv t_2 - t_1$ and the angle brackets denote ensemble averaging. It is to be noted that this ensemble average is equivalent to three independent averages: the average over the arrival times t_j of the pulses, the average over the inclination factors $\mathbf{K}_j$, and the average over the number of pulses per interval N. The instantaneous form of this function for our field of N pulses is

$$V_N^*(\mathbf{r}_1,t_1) V_N(\mathbf{r}_2,t_2) = \sum_{i,j=1}^{N} \Lambda^*(\mathbf{r}_1, t_1 - t_i) \exp[\mathrm{i}\mathbf{K}_i \cdot \mathbf{r}_1] \Lambda(\mathbf{r}_2, t_2 - t_j) \exp[-\mathrm{i}\mathbf{K}_j \cdot \mathbf{r}_2]. \tag{4}$$

We first wish to evaluate the functional form of this quantity when we average over the arrival times t_i. To do so, we express $\Lambda(\mathbf{r},t)$ in terms of its temporal Fourier transform, i.e.

$$\Lambda(\mathbf{r},t) = \int_0^\infty \tilde{\Lambda}(\mathbf{r},\omega) e^{-i\omega t} \mathrm{d}\omega. \tag{5}$$

Our expression (4) may then be written in the form

$$\begin{aligned} V_N^*(\mathbf{r}_1,t_1) V_N(\mathbf{r}_2,t_2) = & \sum_{i,j=1}^{N} \int_0^\infty \int_0^\infty \tilde{\Lambda}^*(\mathbf{r}_1,\omega) \tilde{\Lambda}(\mathbf{r}_2,\omega') \exp[\mathrm{i}\mathbf{K}_i \cdot \mathbf{r}_1] \exp[-\mathrm{i}\mathbf{K}_j \cdot \mathbf{r}_2] \\ & \times \quad \exp[\mathrm{i}\omega(t_1 - t_i)] \exp[-\mathrm{i}\omega'(t_2 - t_j)] \mathrm{d}\omega \mathrm{d}\omega'. \end{aligned} \tag{6}$$

The time average of a function of t_i and t_j over the interval can be written as

$$\langle F(t_i,t_j) \rangle = \frac{1}{T^2} \int_{-T/2}^{T/2} \int_{-T/2}^{T/2} F(t_i,t_j) \mathrm{d}t_i \mathrm{d}t_j. \tag{7}$$

#72209 - $15.00 USD Received 20 June 2006; revised 21 July 2006; accepted 25 July 2006

We may therefore write

$$\langle \exp[-\mathrm{i}(\omega t_i - \omega' t_j)] \rangle = \begin{cases} \mathrm{sinc}[(\omega-\omega')T/2] \equiv f(\omega-\omega'), & i=j, \\ \mathrm{sinc}[\omega T/2]\mathrm{sinc}[\omega' T/2] \equiv g(\omega)g(\omega'), & i \neq j, \end{cases} \tag{8}$$

$$\langle \exp[-\mathrm{i}\omega t_i] \rangle = \mathrm{sinc}[\omega T/2] \equiv g(\omega), \tag{9}$$

where $\mathrm{sinc}[x] \equiv \sin[x]/x$. We may separate our expression (6) into two distinct sums: one for which $i = j$ and one for which $i \neq j$. We may then write

$$\begin{aligned} \langle V_N^*(\mathbf{r}_1,t_1)V_N(\mathbf{r}_2,t_2)\rangle = & \sum_{i=1}^{N} \int_0^\infty \int_0^\infty \tilde{\Lambda}^*(\mathbf{r}_1,\omega)\tilde{\Lambda}(\mathbf{r}_2,\omega')\langle \exp[\mathrm{i}\mathbf{K}_i\cdot(\mathbf{r}_1-\mathbf{r}_2)]\rangle \\ & \times \exp[\mathrm{i}(\omega t_1 - \omega' t_2)] f(\omega-\omega')\mathrm{d}\omega\mathrm{d}\omega' \\ & + \sum_{i\neq j}^{N} \int_0^\infty \int_0^\infty \tilde{\Lambda}^*(\mathbf{r}_1,\omega)\tilde{\Lambda}(\mathbf{r}_2,\omega')\langle \exp[\mathrm{i}(\mathbf{K}_i\cdot\mathbf{r}_1 - \mathbf{K}_j\cdot\mathbf{r}_2)]\rangle \\ & \times \exp[\mathrm{i}(\omega t_1 - \omega' t_2)] g(\omega)g(\omega')\mathrm{d}\omega\mathrm{d}\omega'. \end{aligned} \tag{10}$$

At this point, the angle brackets on the exponentials refer only to averaging over the inclination factors $\mathbf{K}_j$. We now use our probability density function to evaluate this average. We have

$$\langle \exp[\mathrm{i}\mathbf{K}_i\cdot(\mathbf{r}_1-\mathbf{r}_2)]\rangle = \int P(\mathbf{K}_i)\exp[\mathrm{i}\mathbf{K}_i\cdot(\mathbf{r}_1-\mathbf{r}_2)]\mathrm{d}^2K_i = (2\pi)^2\tilde{P}(\mathbf{r}_2-\mathbf{r}_1), \tag{11}$$

$$\langle \exp[\mathrm{i}(\mathbf{K}_i\cdot\mathbf{r}_1 - \mathbf{K}_j\cdot\mathbf{r}_2)]\rangle = (2\pi)^4\tilde{P}^*(\mathbf{r}_1)\tilde{P}(\mathbf{r}_2), \tag{12}$$

where $\tilde{P}(\mathbf{r})$ represents the two-dimensional Fourier transform of the probability density function, defined by

$$\tilde{P}(\mathbf{r}) = \frac{1}{(2\pi)^2}\int P(\mathbf{K})\exp[-\mathrm{i}\mathbf{K}\cdot\mathbf{r}]\mathrm{d}^2K. \tag{13}$$

The sums may then be evaluated, and we find that

$$\begin{aligned} \Gamma_N(\mathbf{r}_1,\mathbf{r}_2,\tau) &= \langle V_N^*(\mathbf{r}_1,t_1)V_N(\mathbf{r}_2,t_2)\rangle \\ &= (2\pi)^2 N \int_0^\infty \int_0^\infty \tilde{\Lambda}^*(\mathbf{r}_1,\omega)\tilde{\Lambda}(\mathbf{r}_2,\omega')\tilde{P}(\mathbf{r}_2-\mathbf{r}_1) \\ &\times \exp[\mathrm{i}(\omega t_1 - \omega' t_2)] f(\omega-\omega')\mathrm{d}\omega\mathrm{d}\omega' \\ &+ (2\pi)^4 N(N-1)\int_0^\infty \int_0^\infty \tilde{\Lambda}^*(\mathbf{r}_1,\omega)\tilde{\Lambda}(\mathbf{r}_2,\omega')\tilde{P}^*(\mathbf{r}_1)\tilde{P}(\mathbf{r}_2) \\ &\times \exp[\mathrm{i}(\omega t_1 - \omega' t_2)] g(\omega)g(\omega')\mathrm{d}\omega\mathrm{d}\omega'. \end{aligned} \tag{14}$$

At this point the integrals are completely independent of the individual realizations of pulses, i.e. the particular values of t_j and $\mathbf{K}_j$ for each pulse, and the only random variable remaining is the number of pulses in the interval. We may average over this quantity as well, to get the mutual coherence function as

$$\Gamma(\mathbf{r}_1,\mathbf{r}_2,\tau) = \sum_{N=0}^{\infty} p(N)\Gamma_N(\mathbf{r}_1,\mathbf{r}_2,\tau), \tag{15}$$

where $p(N)$ is the Poisson distribution. We need the well-established results

$$\sum_{N=0}^{\infty} p(N)N = \overline{N}, \tag{16}$$

$$\sum_{N=0}^{\infty} p(N)N(N-1) = \overline{N}^2. \tag{17}$$

#72209 - $15.00 USD Received 20 June 2006; revised 21 July 2006; accepted 25 July 2006

The mutual coherence function may then be written as

$$\begin{aligned}\Gamma(\mathbf{r}_1,\mathbf{r}_2,\tau) &= (2\pi)^2\overline{N}\int_0^\infty\int_0^\infty \tilde{\Lambda}^*(\mathbf{r}_1,\omega)\tilde{\Lambda}(\mathbf{r}_2,\omega')\tilde{P}(\mathbf{r}_2-\mathbf{r}_1)\\ &\times \exp[\mathrm{i}(\omega t_1-\omega' t_2)]f(\omega-\omega')\mathrm{d}\omega\mathrm{d}\omega'\\ &+ (2\pi)^4\overline{N}^2\int_0^\infty\int_0^\infty \tilde{\Lambda}^*(\mathbf{r}_1,\omega)\tilde{\Lambda}(\mathbf{r}_2,\omega')\tilde{P}^*(\mathbf{r}_1)\tilde{P}(\mathbf{r}_2)\\ &\times \exp[\mathrm{i}(\omega t_1-\omega' t_2)]g(\omega)g(\omega')\mathrm{d}\omega\mathrm{d}\omega'. \end{aligned} \tag{18}$$

Defining the average rate of pulse emission as $\eta=\overline{N}/T$, we may rewrite Eq. (18) in the form

$$\begin{aligned}\Gamma(\mathbf{r}_1,\mathbf{r}_2,\tau) &= (2\pi)^2\eta\int_0^\infty\int_0^\infty \tilde{\Lambda}^*(\mathbf{r}_1,\omega)\tilde{\Lambda}(\mathbf{r}_2,\omega')\tilde{P}(\mathbf{r}_2-\mathbf{r}_1)\\ &\times \exp[\mathrm{i}(\omega t_1-\omega' t_2)]f(\omega-\omega')T\mathrm{d}\omega\mathrm{d}\omega'\\ &+ (2\pi)^4\eta^2\int_0^\infty\int_0^\infty \tilde{\Lambda}^*(\mathbf{r}_1,\omega)\tilde{\Lambda}(\mathbf{r}_2,\omega')\tilde{P}^*(\mathbf{r}_1)\tilde{P}(\mathbf{r}_2)\\ &\times \exp[\mathrm{i}(\omega t_1-\omega' t_2)]g(\omega)Tg(\omega')T\mathrm{d}\omega\mathrm{d}\omega'. \end{aligned} \tag{19}$$

Letting the measurement interval $T\to\infty$, the functions $f(\omega)T$ and $g(\omega)T$ reduce to

$$f(\omega-\omega')T\to 2\pi\delta(\omega-\omega'), \tag{20}$$

$$g(\omega)\to 4\pi\delta^{(e)}(\omega), \tag{21}$$

where $\delta(\omega)$ is the Dirac delta function and $\delta^{(e)}$ is the even half-delta function, defined such that

$$\int_0^\varepsilon \delta^{(e)}(\omega)\mathrm{d}\omega=\frac{1}{2}. \tag{22}$$

By use of these results, the mutual coherence function becomes

$$\begin{aligned}\Gamma(\mathbf{r}_1,\mathbf{r}_2,\tau) &= (2\pi)^3\eta\int_0^\infty \tilde{\Lambda}^*(\mathbf{r}_1,\omega)\tilde{\Lambda}(\mathbf{r}_2,\omega)\tilde{P}(\mathbf{r}_2-\mathbf{r}_1)\exp[-\mathrm{i}\omega\tau]\mathrm{d}\omega\\ &+ (2\pi)^6\eta^2\tilde{\Lambda}^*(\mathbf{r}_1,0)\tilde{\Lambda}(\mathbf{r}_2,0)\tilde{P}^*(\mathbf{r}_1)\tilde{P}(\mathbf{r}_2). \end{aligned} \tag{23}$$

The latter term is the DC-contribution to the field. If we are considering sufficiently narrowband optical signals, it may be safely neglected.

One more simplification will be convenient. We assume that the spatial and temporal parts of the field factorize, i.e. that

$$\Lambda(\mathbf{r},t)=\Theta(\mathbf{r})\Phi(t), \tag{24}$$

so that

$$\tilde{\Lambda}(\mathbf{r},\omega)=\Theta(\mathbf{r})\tilde{\Phi}(\omega). \tag{25}$$

We may then write

$$\Gamma(\mathbf{r}_1,\mathbf{r}_2,\tau)=\eta(2\pi)^3\Theta^*(\mathbf{r}_1)\Theta(\mathbf{r}_2)\tilde{P}(\mathbf{r}_2-\mathbf{r}_1)\int_0^\infty|\tilde{\Phi}(\omega)|^2\exp[-\mathrm{i}\omega\tau]\mathrm{d}\omega. \tag{26}$$

If we consider this field in the space-frequency domain, and consider instead the cross-spectral density $W(\mathbf{r}_1,\mathbf{r}_2,\omega)$ of the field, we have

$$W(\mathbf{r}_1,\mathbf{r}_2,\omega)=\eta(2\pi)^3|\tilde{\Phi}(\omega)|^2\Theta^*(\mathbf{r}_1)\Theta(\mathbf{r}_2)\tilde{P}(\mathbf{r}_2-\mathbf{r}_1), \tag{27}$$

#72209 - $15.00 USD Received 20 June 2006; revised 21 July 2006; accepted 25 July 2006

where

$$W(\mathbf{r}_1,\mathbf{r}_2,\omega)=\frac{1}{2\pi}\int_{-\infty}^{\infty}\Gamma(\mathbf{r}_1,\mathbf{r}_2,\tau)\exp[\mathrm{i}\omega\tau]\mathrm{d}\tau. \tag{28}$$

Equation (27) is the main result of this paper. It demonstrates that the cross-spectral density of our realization of pulses will have a spectrum $|\tilde{\Phi}(\omega)|^2$, an average field profile $\Theta^*(\mathbf{r}_1)$ and a spectral degree of coherence $\tilde{P}(\mathbf{r}_2-\mathbf{r}_1)$. These three functions can be chosen independently of one another, and we may therefore construct a realization of a partially coherent field which has quite general spatial and temporal coherence.

It is to be noted that our results are not completely general, i.e. there exist partially coherent fields which cannot be realized by this random pulse technique. In particular, there exist fields whose spatial and temporal coherence properties are not factorizable, and there also exist fields whose spectral degree of coherence is frequency dependent. Nevertheless, our method provides an excellent tool for creating realizations of quite arbitrary spatial and temporal coherence.

3. Intensity fluctuations of partially coherent field realizations

We have as yet only considered the second-order coherence properties of the optical field. It is worthwhile, however, to investigate the fourth-order coherence properties achievable by our simulation method as well, as intensity fluctuations of an optical signal (in particular, its scintillation index [15]) play an important role in optical communications.

The scintillation index is defined as [15, Sec. 1.7]

$$\sigma_I^2(\mathbf{r})=\frac{\langle I(\mathbf{r},t)^2\rangle}{\langle I(\mathbf{r},t)\rangle^2}-1, \tag{29}$$

where $I(\mathbf{r},t)=\langle|V(\mathbf{r},t)|^2\rangle$ is the intensity of the field which is on average independent of time. The quantity $\langle I(\mathbf{r},t)\rangle^2$ can be derived from the results of the previous section, so we focus on the quantity $\langle I(\mathbf{r},t)^2\rangle$. Using our collection of pulses over a finite interval T again, we have

$$\langle I_N(\mathbf{r},t)^2\rangle=\langle V_N^*(\mathbf{r},t)V_N^*(\mathbf{r},t)V_N(\mathbf{r},t)V_N(\mathbf{r},t)\rangle, \tag{30}$$

where $V_N(\mathbf{r},t)$ is defined by Eq. (2). Looking at the temporal Fourier decomposition of this equation, we find that

$$\begin{aligned}\langle I_N(\mathbf{r},t)^2\rangle &= \sum_{ijkl}^{N}\int_0^\infty\int_0^\infty\int_0^\infty\int_0^\infty\tilde{\Lambda}^*(\mathbf{r},\omega_1)\tilde{\Lambda}^*(\mathbf{r},\omega_2)\\ &\times\ \tilde{\Lambda}(\mathbf{r},\omega_3)\tilde{\Lambda}(\mathbf{r},\omega_4)\exp\left[\mathrm{i}t(\omega_1+\omega_2-\omega_3-\omega_4)\right]\\ &\times\ \langle\exp\left[-\mathrm{i}(\omega_1t_i+\omega_2t_j-\omega_3t_k-\omega_4t_l)\right]\rangle\\ &\times\ \langle\exp\left[\mathrm{i}\mathbf{r}\cdot(\mathbf{K}_i+\mathbf{K}_j-\mathbf{K}_k-\mathbf{K}_l)\right]\rangle\mathrm{d}\omega_1\mathrm{d}\omega_2\mathrm{d}\omega_3\mathrm{d}\omega_4.\end{aligned} \tag{31}$$

There are N^4 terms to the summation, but most of them result in either a zero-frequency contribution which will be neglected or a negative-frequency term which is identically zero. The only non-zero terms are those for which

$$\begin{aligned} i=j=k=l=\alpha, &\qquad N \text{ terms},\\ \alpha=i=k\neq j=l=\beta &\qquad N(N-1) \text{ terms},\\ \alpha=i=l\neq j=k=\beta &\qquad N(N-1) \text{ terms}.\end{aligned}$$

These averages can be calculated as in the previous section. We have

$$\langle\exp\left[-\mathrm{i}(\omega_1+\omega_2-\omega_3-\omega_4)t_\alpha\right]\rangle=2\pi\delta(\omega_1+\omega_2-\omega_3-\omega_4),$$

#72209 - $15.00 USD Received 20 June 2006; revised 21 July 2006; accepted 25 July 2006

(32)

$$\langle \exp[-\mathrm{i}(\omega_1-\omega_3)t_\alpha]\rangle\langle \exp\left[-\mathrm{i}(\omega_2-\omega_4)t_\beta\right]\rangle = (2\pi)^2\delta(\omega_1-\omega_3)\delta(\omega_2-\omega_4), \tag{33}$$

$$\langle \exp[-\mathrm{i}(\omega_1-\omega_4)t_\alpha]\rangle\langle \exp\left[-\mathrm{i}(\omega_2-\omega_3)t_\beta\right]\rangle = (2\pi)^2\delta(\omega_1-\omega_4)\delta(\omega_2-\omega_3). \tag{34}$$

Similarly, for the spatial average, we have

$$\langle \exp[\mathrm{i}(\mathbf{K}_i+\mathbf{K}_j-\mathbf{K}_k-\mathbf{K}_l)\cdot\mathbf{r}]\rangle = \begin{array}{ll} (2\pi)^2\tilde{P}(0)=1, & i=j=k=l=\alpha, \\ (2\pi)^4(\tilde{P}(0))^2=1, & \alpha=i=k\neq j=l=\beta, \\ (2\pi)^4(\tilde{P}(0))^2=1, & \alpha=i=l\neq j=k=\beta. \end{array} \tag{35}$$

Our expression for the intensity fluctuations takes on the form

$$\begin{aligned} \langle I(\mathbf{r},t)^2\rangle &= 2\pi\eta\int_0^\infty\int_0^\infty\int_0^\infty \tilde{\Lambda}^*(\mathbf{r},-\omega_2+\omega_3+\omega_4)\tilde{\Lambda}^*(\mathbf{r},\omega_2) \\ &\times \tilde{\Lambda}(\mathbf{r},\omega_3)\tilde{\Lambda}(\mathbf{r},\omega_4)\mathrm{d}\omega_2\mathrm{d}\omega_3\mathrm{d}\omega_4 \\ &+ (2\pi)^2 2\eta^2\int_0^\infty\int_0^\infty |\tilde{\Lambda}(\mathbf{r},\omega_1)|^2|\tilde{\Lambda}(\mathbf{r},\omega_2)|^2\mathrm{d}\omega_1\mathrm{d}\omega_2. \end{aligned} \tag{36}$$

We again factorize our field into a temporal and spatial part. Noting that the frequency dependence of the first term is a convolution, and the second part is simply $\langle I(\mathbf{r},t)\rangle^2$, we may write

$$\langle I(\mathbf{r},t)^2\rangle = \eta|\Theta(\mathbf{r})|^4\int_{-\infty}^\infty |\Phi(t)|^4\mathrm{d}t + 2\langle I(\mathbf{r},t)\rangle^2. \tag{37}$$

On substitution into the scintillation index, we readily find that

$$\sigma_I^2 = \frac{1}{\eta}\frac{\int_{-\infty}^\infty|\Phi(t)|^4\mathrm{d}t}{|\int_\infty^\infty|\Phi(t)|^2\mathrm{d}t|^2}+1. \tag{38}$$

In the limit $\eta\to\infty$, i.e. a large rate of pulse emission, we find that $\sigma_I\sim 1$. This result is consistent with a light field said to be *chaotic* or *Gaussian* [16, chapter 3]. Our simulation method therefore cannot produce a pure coherent laser field. However, partially coherent fields derived from laser light, for instance by passing coherent light through a rotating ground glass plate, are well-known to be chaotic [17] and our simulation method will reliably simulate many partially coherent field configurations.

Although $\sigma_I^2=1$ is the ideal limit for our simulation method, for small values of η (small rate of pulse emission) the value of σ_I^2 can be much higher. We can estimate how large η must be to reach the ideal limit by considering Gaussian pulses,

$$\Phi(t) = \frac{1}{\sqrt{\pi}\sigma_t}\exp[-t^2/\sigma_t^2]. \tag{39}$$

On substitution into our formula (38), we readily find that

$$\sigma_I^2 = \frac{1}{\sqrt{\pi}}\frac{1}{\eta\sigma_t}+1. \tag{40}$$

We can approach the ideal value of $\sigma_I^2\sim 1$ by taking $\eta\sigma_t$ to be sufficiently large.

4. Examples

We now demonstrate the use of the field generator by numerical examples.

#72209 - $15.00 USD Received 20 June 2006; revised 21 July 2006; accepted 25 July 2006

4.1. *Gaussian Schell-model fields*

We consider fields of Gaussian intensity profile and Gaussian spatial correlation, known as Gaussian Schell-model fields [3, Sec. 5.2.2]. The mutual coherence function of such fields may be written as

$$\Gamma(\mathbf{r}_1,\mathbf{r}_2,\tau) = \gamma(\tau)\sqrt{I(\mathbf{r}_1)}\sqrt{I(\mathbf{r}_2)}\mu(\mathbf{r}_2-\mathbf{r}_1), \tag{41}$$

where $I(\mathbf{r})$ is the average field intensity,

$$I(\mathbf{r}) = \exp[-\mathbf{r}^2/2\sigma_I^2], \tag{42}$$

σ_I being the beam width, $\mu(\mathbf{r}_2-\mathbf{r}_1)$ is the spatial correlation function (equivalent to the spectral degree of coherence in the frequency domain),

$$\mu(\mathbf{r}_2-\mathbf{r}_1) = \exp[-(\mathbf{r}_2-\mathbf{r}_1)^2/2\sigma_g^2], \tag{43}$$

σ_g being the correlation length, and $\gamma(\tau)$ is the temporal coherence function, to be taken as Lorentzian or Gaussian. On comparison with Eq. (27), it can be seen that our field generator should generate a Gaussian Schell-model field if we take $\sqrt{I(\mathbf{r})} = \sqrt{\eta(2\pi)^3}\Theta(\mathbf{r})$, $\tilde{P}(\mathbf{r}) = \mu(\mathbf{r})$, and take $|\tilde{\Phi}(\omega)|^2$ to be the temporal Fourier transform of $\gamma(\tau)$. Figure 1 illustrates the intensity of the field generated by our simulation method for several realizations, with $\sigma_I = 2\,\text{cm}$, $\sigma_g = 1\,\text{cm}$, and Gaussian spectrum of center frequency $1\times10^{15}\,\text{Hz}$ and 1% bandwidth. The average pulse rate is taken to be 5 pulses/cycle. The pictures show the gradual evolution of the field in time; the frames are each separated by 5 periods at the center frequency.

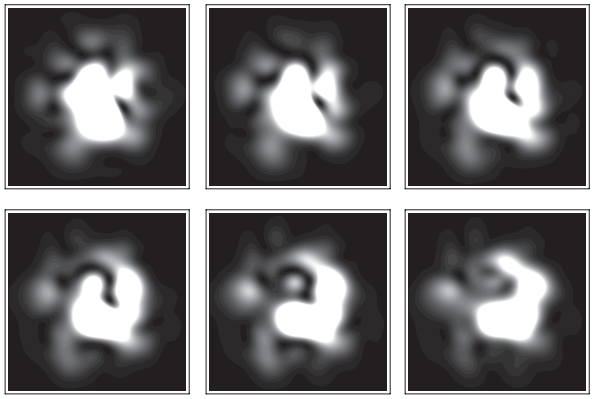

Fig. 1. Illustrating several realizations of the intensity of the field generated by the method with $\sigma_I = 2\,\text{cm}$, $\sigma_g = 1\,\text{cm}$, and Gaussian spectrum of center frequency $1\times10^{15}\,\text{Hz}$ and 1% bandwidth. The pictures show the gradual evolution of the field in time; the frames are each separated by 5 periods at the center frequency. The window size is 10 cm on a side.

To be a valid technique for generating realizations, the field must possess the proper prescribed average properties. Figure 2 illustrates the average intensity of the field, taken over 50 instantaneous values of the field each separated by 20 periods at the center frequency. Part (a) shows the cross-section of the beam, while (b) shows the cross-section of the beam along the line $y = 0$. The ideal Gaussian is shown as a dashed line, and it can be seen that there is excellent agreement. Convergence could be further improved by extending the duration of the time average.

The spatial correlation properties can also be numerically calculated to test the technique. Figure 3 shows the average spatial correlation properties, taken over 50 instantaneous values of the field each separated by 20 periods at the center frequency. The spatial correlation properties

#72209 - $15.00 USD Received 20 June 2006; revised 21 July 2006; accepted 25 July 2006

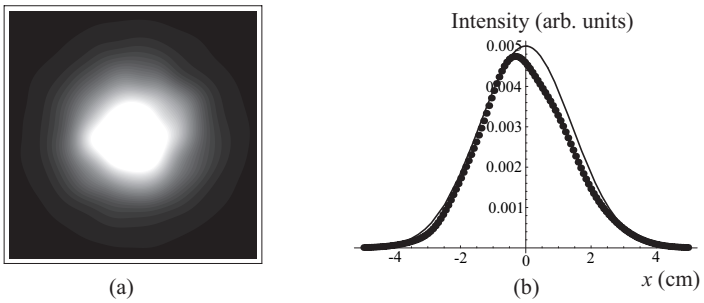

Fig. 2. Illustrating the average intensity of the field (a) in the source plane and (b) through a cross-section of the source plane. The dots indicate the numerically calculated result; the solid line indicates the expected result of Eq. (41). The average is taken over 50 instantaneous values of the field, each separated by 20 periods at the center frequency. All other parameters are as in Fig. 1.

were calculated at points $+x$, $-x$ along the line $y = 0$. The circles represent the results generated from our realization, while the dashed line represents the ideal Gaussian Schell-model case. Again it can be seen that there is excellent agreement.

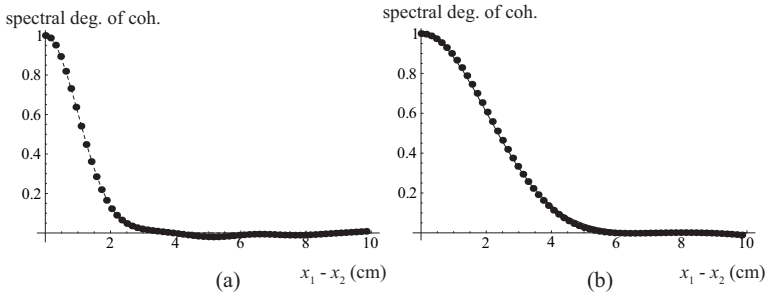

Fig. 3. Illustrating the spectral degree of coherence of the field as calculated using 50 instantaneous values of the field, each separated by 20 periods at the center frequency. For (a), $\sigma_g = 1\,\mathrm{cm}$, while for (b), $\sigma_g = 2\,\mathrm{cm}$. The dashed lines indicate the expected result of Eq. (41).

The average temporal correlation properties of the field can also be numerically calculated. Figure 4 shows the complex degree of coherence $\gamma(\tau)$ calculated at the center of a coherent Gaussian beam, for a Gaussian and Lorentian lineshape. Again there is excellent agreement between the results of the simulation and the expected average behavior.

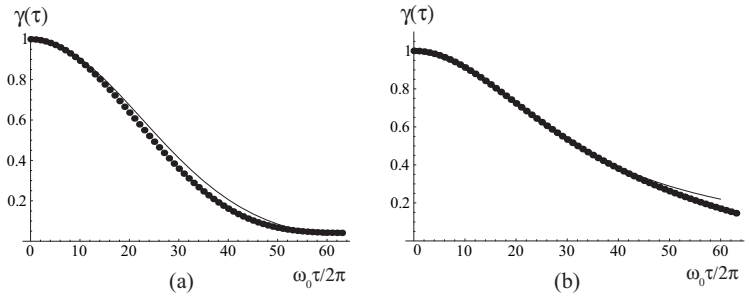

Fig. 4. Illustrating the temporal coherence function calculated by time averaging. The solid lines indicate the analytic prediction. For (a), the function is Gaussian, while for (b), the function is Lorentzian.

#72209 - $15.00 USD Received 20 June 2006; revised 21 July 2006; accepted 25 July 2006

4.2. Propagation through random phase screens

We now consider the propagation of our partially coherent field realizations through random phase screens. Such phase screens are extensively used to model the effects of beam propagation through weak turbulence [18]. The field must be propagated from the source plane to the plane of the phase screen, and then propagated beyond it to a detector plane. Though such Fresnel-type propagation has of course been done many times, is it uncommon to see it in the time domain, so we briefly summarize the technique. We may use Huygens' principle to express the propagation of the field $V(\mathbf{r}',t)$ from the plane $z=0$ in the form

$$V(\mathbf{r},t) = \int\int_{z=0} \frac{V_0(\mathbf{r}',t-R/c)}{R} \mathrm{d}^2 r', \tag{44}$$

where $V_0(\mathbf{r}',t)$ is the field in the source plane $z=0$, $R=|\mathbf{r}-\mathbf{r}'|$ is the source point-field point distance, and the integration is carried out over the source plane. For quasi-monochromatic fields such as we are considering, we may separate the source field into the components

$$V(\mathbf{r},t) = \exp[\mathrm{i}\omega_0 t] F_0(\mathbf{r},t), \tag{45}$$

where ω_0 is the central frequency of oscillation of the source and $F_0(\mathbf{r},t)$ is the slowly-varying piece of the source field. We may then write

$$V(\mathbf{r},t) = \exp[\mathrm{i}\omega_0 t] \int\int_{z=0} \exp[-\mathrm{i}\omega_0 R/c] \frac{F_0(\mathbf{r}',t-R/c)}{R} \mathrm{d}^2 r'. \tag{46}$$

We are also primarily interested in paraxial fields, for which

$$R = |\mathbf{r}-\mathbf{r}'| \approx z + \frac{1}{2}\frac{(x-x')^2+(y-y')^2}{z}. \tag{47}$$

The field may then be simplified to the form

$$\begin{aligned} V(\mathbf{r},t) &= \frac{\exp[\mathrm{i}\omega_0 t]\exp[-\mathrm{i}\omega_0 z/c]}{z} \int\int_{z=0} \exp\left[-\mathrm{i}\frac{\omega_0}{2c}\frac{(x-x')^2+(y-y')^2}{z}\right] \\ &\times F_0\left[\mathbf{r}', t-\frac{1}{c}\left(z+\frac{1}{2}\frac{(x-x')^2+(y-y')^2}{z}\right)\right] \mathrm{d}^2 r'. \end{aligned} \tag{48}$$

Since the function F_0 is assumed to be slowly-varying with respect to time and paraxial, the spatial argument which depends on the tranverse coordinates will be negligible compared to the other terms. We may simplify our field calculation to the form

$$V(\mathbf{r},t) = \frac{\exp[\mathrm{i}\omega_0 \hat{t}]}{z} \int\int_{z=0} \exp\left[-\mathrm{i}\frac{\omega_0}{2c}\frac{(x-x')^2+(y-y')^2}{z}\right] F_0(\mathbf{r}',\hat{t}) \mathrm{d}^2 r', \tag{49}$$

where $\hat{t} \equiv t - z/c$. The field in any plane of constant z is therefore simply the time-shifted Fresnel transform of the field in the source plane, and can be calculated straightforwardly with a fast Fourier transform.

We study the response of the partially coherent field on propagation through a Gaussian random phase screen with power spectrum

$$S(K) = \phi_0^2 \exp\left[-k^2 L_0^2/4\right], \tag{50}$$

where L_0 is the outer scale of the phase screen. Such a screen is a poor model for quantitative studies of atmospheric turbulence (in such cases more sophisticated spectral models exist [9]),

#72209 - $15.00 USD Received 20 June 2006; revised 21 July 2006; accepted 25 July 2006

but will suffice for a brief illustration of partially coherent field propagation through random media. The screens are generated by the method described in Ref. [18]. We take as screen parameters $\phi_0^2 = 1$, $L_0 = 15\,\text{cm}$ and the screen is located at $z = 1.0\,\text{km}$. A spatially coherent field with $\sigma_I = 2\,\text{cm}$ is propagated through this screen and to a detector at $z = 2\,\text{km}$; the intensity at the detector is shown in Fig. 5(a). It can be seen that the spot has been aberrated by the phase screen and, perhaps more important, is no longer centered on the center of the detector plane. This is an example of beam wander; it is to be noted that if the beam wanders sufficiently from the axis, it may not illuminate the detector at all, resulting in information loss (a 'miss'). Temporal fluctuations of the coherent field do not fix the problem; as illustrated in Fig. 5(b), over a 200 cycle time average of the field, the spot shape and position remain essentially unchanged.

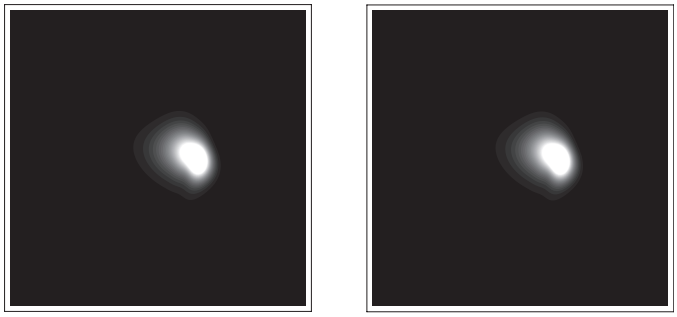

(a) (b)

Fig. 5. Illustrating (a) the instantaneous intensity and (b) the average intensity of a spatially coherent field after propagating through a Gaussian random phase screen at $z = 1.0\,\text{km}$, with the detector plane at $z = 2\,\text{km}$. Here $L_0 = 15\,\text{cm}$ and $\phi_0^2 = 1$.

We now consider the propagation of a partially coherent field with $\sigma_g = 1\,\text{cm}$ through the same phase screen. As illustrated in Fig. 6(a), this field is also significantly distorted by the phase screen. However, some field intensity is still present in the center of the detector plane. When a long time average is taken, as shown in Fig. 6(b), we see that there is still a tendency for the field to 'wander' from the center of the screen, but an appreciable amount of field intensity remains near the center of the detector plane.

These results suggest the following picture for the improved propagation characteristics of partially coherent fields in turbulence, as illustrated in Fig. 7. A coherent laser essentially propagates its energy through a single coherent mode, which is subject to distortion on propagation through the inhomogeneous medium. The signal may or may not arrive fully at the detector, and will have suffered degradation due to diffraction. The partially coherent beam sends its energy through multiple (independent) modes, each of which propagates differently in the turbulent medium. Although any individual mode may not arrive cleanly at the detector, it is likely that at least one will make the journey. For our particular method of generating realizations, the modes are the individual pulses, each of which has a different 'angle of attack' (value of $\mathbf{K}_j$) into the phase screen.

5. Conclusions

We have derived a new method of generating realizations of partially coherent fields of nearly arbitrary spatial and temporal coherence. The method was demonstrated for Gaussian Schell-model fields of different degrees of spatial and temporal coherence, and the numerically calculated average properties agree well with the predicted analytical results. The method was also used to gain some insight into the propagation of partially coherent beams through random

#72209 - $15.00 USD Received 20 June 2006; revised 21 July 2006; accepted 25 July 2006

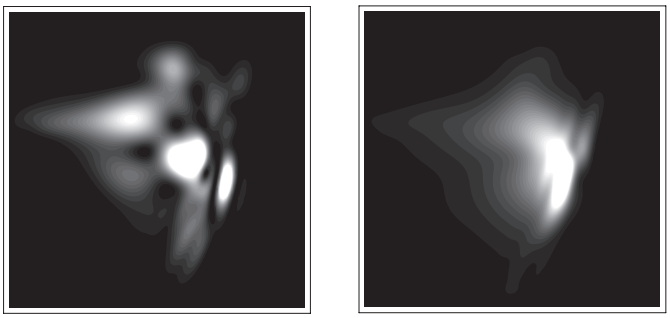

(a) (b)

Fig. 6. Illustrating (a) the instantaneous intensity and (b) the average intensity of a partially coherent field with $\sigma_g = 1\,\text{cm}$ after propagating through a Gaussian random phase screen at $z = 1.0\,\text{km}$, with the detector plane at $z = 2\,\text{km}$. Here $L_0 = 15\,\text{cm}$ and $\phi_0^2 = 1$.

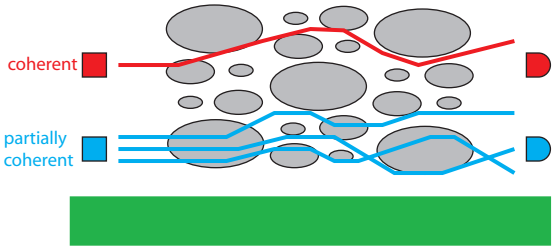

Fig. 7. A qualitative explanation of the behavior of partially coherent beams in turbulence. A coherent laser essentially propagates its energy through a single coherent mode, which is subject to distortion on propagation through the inhomogeneous medium. The partially coherent beam sends its energy through multiple (independent) modes, each of which propagates differently in the turbulent medium.

phase screens, which could be used as a rough model for atmospheric turbulence. It is expected that the ability to study the behavior of fluctuating fields on many time scales (center frequency, bandwidth, rate of turbulence fluctuations, detector response) will provide useful insight into the behaviors of many coherence-related phenomena.

It is to be noted that this method can also be used as an educational tool. Coherence theory is often difficult for the beginner to understand. This method of generating realizations can be used as an additional visual/conceptual aid for the student of optical coherence, as well as a technique for generating unique homework assignments – each student could be given a realization of a field and asked to determine its spatial and temporal properties.

Acknowledgements

The research was supported by the US Air Force Office of Scientific Research under grant FA 9550-05-1-0288.

#72209 - $15.00 USD Received 20 June 2006; revised 21 July 2006; accepted 25 July 2006